

DRAFT VERSION SEPTEMBER 19, 2024

Typeset using L^AT_EX default style in AASTeX631

Exploration of Stellar Variability in 20-second Cadence TESS Data

COOPER DEVANE-PRUGH,¹ CARMEN MICHAUD,¹ JAMIE TAYAR,¹ DANIEL J. STEVENS,² RACHAEL BEATON,³
JOHANNA TESKE,⁴ AND JENNIFER VAN SADERS⁵¹*Department of Astronomy, University of Florida, Gainesville, FL 32611, USA*²*Department of Physics & Astronomy, University of Minnesota Duluth, Duluth, MN 55812, USA*³*Space Telescope Science Institute, Baltimore, MD 21218, USA*⁴*Carnegie Earth and Planets Laboratory, Washington, DC 20015, USA*⁵*Institute for Astronomy, University of Hawai‘i, Honolulu, HI 96822, USA*

ABSTRACT

The introduction of TESS’s 20-second cadence mode has given us the opportunity to examine the variation of stellar flux on shorter timescales than ever before. While we find no previously undetected variability at these timescales, we find oscillations outside of the published instability strip in TIC 349902873. We also quantify the stellar variability on specific timescales using the combined differential photometric precision (CDPP). We developed a light-curve creation pipeline for 57 bright stars in TESS’ SCVZ across the HR diagram with extant spectra. From the light curves, we reproduced the scaling previously seen between CDPP and magnitude at all timescales in our data set. We also find a potential correlation between CDPP on the shortest timescales and surface gravity, which may be related to convection and oscillations and impact the relative detectability of exoplanet features.

Keywords: Stellar photometry(1620) – Variable stars(1761)

1. DATA SET

To explore the novel 20-second cadence data from TESS, we used the SDSS APOGEE survey (DR16 pipeline, MJD = 58932 results; Holtzman et al. 2018) to select a sample of stars located in the TESS Southern Continuous Viewing Zone. These 57 stars represent 19 interesting points of evolution, including a range of masses and phases along the main sequence, subgiant, and giant branch (Figure 1). We obtained 12-13 sectors of TESS Cycle 3 observations for each star (MAST Team 2021).

TESS’s SPOC pipeline provides light curves generated via Simple Aperture Photometry (SAP) and Presearch Data Conditioning SAP (Jenkins et al. 2016). However, these light curves retain significant instrumental systematics that are sector dependent (Avalone et al. 2022). Therefore, we implemented a pipeline¹ (DeVane-Prugh & Tayar 2024) that removes NaN values and points with non zero quality flags and sigma clips outliers greater than 5σ . We clip the first and last days of each sector, as well as one day around TESS safe modes and discontinuities, where systematic effects are most prevalent. The sectors are median-normalized, then stitched together into a single light curve. We ultimately removed a handful of stars from our sample that showed evidence of crowding. We compare our light curves to others (Nandakumar et al. 2022) and find consistent results.

2. CDPP METHODS

The combined differential photometric precision was developed for the Kepler mission to assess photometric noise in light curves (Christiansen et al. 2012). Photometric noise is non-uniform and non-stationary, and thus a photometric noise time series is generated by the Transiting Planet Search (TPS) module in the official TESS pipeline for each target (Jenkins et al. 2016). CDPP is the root mean square of this time series on timescales relevant to transiting planets. It represents the ease with which planet transit signatures can be detected in a given target (Christiansen et al. 2012), and is therefore a useful characterization of photometric variability.

¹ DOI: 10.5281/zenodo.13363434

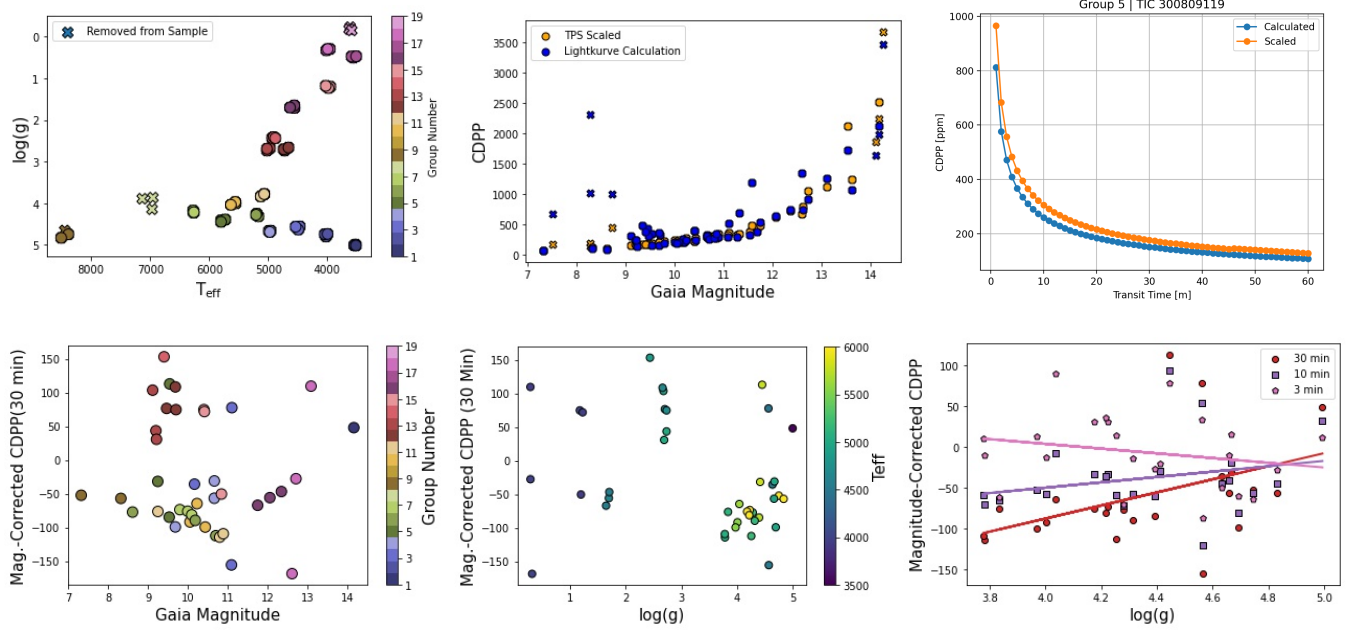


Figure 1. For our sample (**Top Left**) we replicate the expected scaling between CDPP and magnitude (**Top Middle**) and show these scalings as a function of timescale (**Top Right**). Once we correct for the scaling with brightness (**Bottom Left**), we search for any residual correlations with stellar properties (**Bottom Middle**) and find that the CDPP as a function of surface gravity depends on the timescale of interest (**Bottom Right**).

The official TPS module uses a wavelet-based algorithm to determine the signal-to-noise ratio for a specific time. However, there is a “sgCDPP proxy algorithm” in `lightcurve` that can be used to estimate CDPP (Gilliland et al. 2011; Cleve et al. 2016; Lightcurve Collaboration et al. 2018). This implementation first removes low frequency signals using a Savitzky-Golay filter, σ clips the data, then computes the standard deviation of a running mean with a window length equal to the desired transit duration. We calculated CDPP using the proxy algorithm in `lightcurve` and reproduce the expected trend of CDPP increasing with magnitude (Figure 1, top middle).

Alternatively, Christiansen et al. (2012) showed that one can estimate ($CDPP_{eff}$) for a desired duration (t_{dur}) by scaling the CDPP value from the official pipeline:

$$CDPP_{eff} = \sqrt{t_{CDPP}/t_{dur}} \times CDPP_N, \quad (1)$$

where t_{CDPP} is the time from the official pipeline closest to t_{dur} , and $CDPP_N$ is the official CDPP value corresponding to that timescale (Christiansen et al. 2012). For TESS targets, CDPP is calculated by the TPS pipeline for 30-min, 1-hour, and 2-hr transit times. For our study, we calculate $CDPP_{eff}$ for timescales between 1 min and 1 hr, in 1-min intervals, using the 30 min and 1 hr CDPP values as appropriate.

Figure 1 (top right) shows that we recover similar trends for the scaled effective CDPP and `lightcurve`-calculated CDPP for TIC 300809119, a solar-like target, at each t_{dur} , although the actual values may be slightly offset, and there is often a “bump” in the scaled CDPP near the 45-min mark due to the transition in $CDPP_N$ values.

3. MAGNITUDE CORRECTIONS

To look for trends in CDPP with other stellar parameters, we first correct for the magnitude dependence. Following Kunimoto et al. (2022), we fit a curve with three components,

$$\sigma = a + b \times 10^{0.2(G-10)} + c \times 10^{0.4(G-10)} \quad (2)$$

where G is the *Gaia* magnitude. We use `scipy`’s curve fitting routines to determine the component values for our calculated 3, 10, and 30 minute CDPP values. We exclude a handful of outliers outside of one standard deviation from the plots, including TIC 349902873, a hybrid p- and g-mode pulsator (Garcia et al. 2022) that lies outside any published instability strip.

4. RESULTS

We show in Figure 1 that we are able to measure the CDPP for the stars in our sample, and that we are able to reproduce the published scalings between CDPP and magnitude. Given that these data were taken at 20-second cadence, we can also compute a CDPP on a variety of timescales for our stars, and in general we find a trend towards greater relative variation on shorter timescales (top right).

Using our sample of stars across the HR diagram, we search for additional trends with the stellar parameters by computing the difference between the measured CDPP and the average predicted CDPP for a star of a given magnitude (bottom left). We do not find strong trends with metallicity or stellar temperature, but we do find a trend with surface gravity. If the enhanced CDPP is due to intrinsic stellar variation, we expect that the trend with surface gravity will depend on the timescale on which CDPP is measured. We show in the final panel of Figure 1 (bottom right) that this is indeed the case.

5. CONCLUSIONS

We show here that TESS’s 20s-cadence data is reliable for stars across the HR diagram. In general, we see no unexpected short-timescale variations for stars of any particular evolutionary phase. We do note that the amount of variation in a star’s light curve, as measured by its CDPP, depends on the apparent magnitude of the star, the surface gravity of the star, and the timescale on which the CDPP is being measured.

As CDPP is often used as a metric for describing how easily the features of an exoplanet transit can be identified, we emphasize that there is an increase in the CDPP for G-dwarfs over K- and M-dwarfs at timescales of a few minutes, which may be relevant for studies of ingress and egress shapes and the detection of atmospheric features on the limb. We therefore suggest that further consideration of the stellar convective and oscillation timescales may be necessary for detailed exoplanetary investigations.

6. ACKNOWLEDGEMENTS

C. D-P., C.M., and J.T. acknowledge support from 80NSSC23K0143. This research made use of Lightkurve, a Python package for Kepler and TESS data analysis (Lightkurve Collaboration, 2018). We utilize data from SDSS (<https://www.sdss.org/collaboration/citing-sdss/>)

REFERENCES

- Avallone, E. A., Tayar, J. N., van Saders, J. L., et al. 2022, *The Astrophysical Journal*, 930, 7, doi: [10.3847/1538-4357/ac60a1](https://doi.org/10.3847/1538-4357/ac60a1)
- Christiansen, J. L., Jenkins, J. M., Caldwell, D. A., et al. 2012, *Publications of the Astronomical Society of the Pacific*, 124, 1279, doi: [10.1086/668847](https://doi.org/10.1086/668847)
- Cleve, J. E. V., Howell, S. B., Smith, J. C., et al. 2016, *Publications of the Astronomical Society of the Pacific*, 128, 075002, doi: [10.1088/1538-3873/128/965/075002](https://doi.org/10.1088/1538-3873/128/965/075002)
- DeVane-Prugh, C., & Tayar, J. 2024, *Data for Exploration of Stellar Variability in 20-second Cadence TESS Data*, Zenodo, doi: [10.5281/zenodo.13363434](https://doi.org/10.5281/zenodo.13363434)
- Garcia, S., Van Reeth, T., De Ridder, J., & Aerts, C. 2022, *A&A*, 668, A137, doi: [10.1051/0004-6361/202244365](https://doi.org/10.1051/0004-6361/202244365)
- Gilliland, R. L., Chaplin, W. J., Dunham, E. W., et al. 2011, *The Astrophysical Journal Supplement Series*, 197, 6, doi: [10.1088/0067-0049/197/1/6](https://doi.org/10.1088/0067-0049/197/1/6)
- Holtzman, J. A., Hasegawa, S., Shetrone, M., et al. 2018, *The Astronomical Journal*, 156, 125, doi: [10.3847/1538-3881/aad4f9](https://doi.org/10.3847/1538-3881/aad4f9)
- Jenkins, J. M., Twicken, J. D., McCauliff, S., et al. 2016, in *Society of Photo-Optical Instrumentation Engineers (SPIE) Conference Series*, Vol. 9913, *Software and Cyberinfrastructure for Astronomy IV*, ed. G. Chiozzi & J. C. Guzman, 99133E, doi: [10.1117/12.2233418](https://doi.org/10.1117/12.2233418)
- Kunimoto, M., Winn, J., Ricker, G. R., & Vanderspek, R. K. 2022, *The Astronomical Journal*, 163, 290, doi: [10.3847/1538-3881/ac68e3](https://doi.org/10.3847/1538-3881/ac68e3)
- Lightkurve Collaboration, Cardoso, J. V. d. M., Hedges, C., et al. 2018, *Lightkurve: Kepler and TESS time series analysis in Python*, *Astrophysics Source Code Library*. <http://ascl.net/1812.013>
- MAST Team. 2021, *TESS "Fast" Light Curves - All Sectors*, STScI/MAST, doi: [10.17909/t9-st5g-3177](https://doi.org/10.17909/t9-st5g-3177)
- Nandakumar, S., Barbieri, M., & Tregloan-Reed, J. 2022, *Astronomische Nachrichten*, 343, doi: [10.1002/asna.20220034](https://doi.org/10.1002/asna.20220034)